Full Length Article

Abnormal clot microstructure formed in blood containing HIT-like antibodies

Bethan R. Thomas[a], Rebecca J. Hambly[a], John W. Weisel[b], Lubica Rauova[b,c], Nafiseh Badiei[d], M. Rowan Brown[d], Catherine A. Thornton[a], P. Rhodri Williams[d], Karl Hawkins[a,*]

[a] Swansea University Medical School, Swansea University, Swansea, UK
[b] University of Pennsylvania School of Medicine, PA, USA
[c] Children's Hospital of Philadelphia, PA, USA
[d] College of Engineering, Swansea University, Swansea, UK

ABSTRACT

Introduction: Thrombosis is a severe and frequent complication of heparin-induced thrombocytopenia (HIT). However, there is currently no knowledge of the effects of HIT-like antibodies on the resulting microstructure of the formed clot, despite such information being linked to thrombotic events. We evaluate the effect of the addition of pathogenic HIT-like antibodies to blood on the resulting microstructure of the formed clot.

Materials and methods: Pathogenic HIT-like antibodies (KKO) and control antibodies (RTO) were added to samples of whole blood containing Unfractionated Heparin and Platelet Factor 4. The formed clot microstructure was investigated by rheological measurements (fractal dimension; d_f) and scanning electron microscopy (SEM), and platelet activation was measured by flow cytometry.

Results and conclusions: Our results revealed striking effects of KKO on clot microstructure. A significant difference in d_f was found between samples containing KKO ($d_f = 1.80$) versus RTO ($d_f = 1.74$; $p < 0.0001$). This increase in d_f was often associated with an increase in activated platelets. SEM images of the clots formed with KKO showed a network consisting of a highly branched and compact arrangement of thin fibrin fibres, typically found in thrombotic disease. This is the first study to identify significant changes in clot microstructure formed in blood containing HIT-like antibodies. These observed alterations in clot microstructure can be potentially exploited as a much-needed biomarker for the detection, management and monitoring of HIT-associated thrombosis.

1. Introduction

Heparin-induced thrombocytopenia (HIT) associated thrombosis is an adverse reaction to heparin therapy with an associated mortality rate of approximately 20% [1]. Rapid and accurate diagnosis is crucial as false diagnosis can expose thrombocytopenic patients to alternative anticoagulants resulting in a risk of major bleeding [2,3]. In HIT, negatively charged heparin polysaccharides bind to positively charged Platelet Factor 4 (PF4) released by activated platelets to form ultra-large complexes (ULCs). ULCs are then identified as an antigen by the immune system, leading to the production of specific antibodies that bind to these ULCs and activate platelets, monocytes and other vascular cells through FcγRIIA [1,4]. Monocyte activation leads to the expression of tissue factor and subsequent generation of thrombin, and activated platelets release additional stores of PF4, which not only

perpetuates the cycle but creates the extreme pro-thrombotic environment in which blood clots associated with HIT are formed [2,5,6].

Abnormal fibrin clot microstructure is widely reported to play an important role in the pathophysiology of pro-thrombotic disease and has clinical implications in the diagnosis and treatment of thrombosis [7]. For example, samples of blood obtained from pro-thrombotic patients, such as patients with premature coronary arterial disease, venous thromboembolism, and ischemic stroke, have been demonstrated to produce "abnormal" clots with a more compact fibrin network of relatively thin, highly branched fibres [8–10]. Moreover, a structural biomarker of haemostasis, the fractal dimension, has detected abnormal clotting in patients with venous thromboembolism, despite those patients being administered warfarin [11]. However, microstructural studies of blood clots associated with HIT have not been reported, even though such analysis could be informative for understanding and

* Corresponding author at: Centre for NanoHealth, Swansea University Medical School, Swansea University, Singleton Park, Swansea, UK.
E-mail address: K.M.Hawkins@swansea.ac.uk (K. Hawkins).

potentially diagnosing the thrombosis accompanying HIT. Herein we investigate fibrin clot microstructure in whole blood clots formed in the presence of KKO, a known pathogenic HIT-like monoclonal antibody to PF4-heparin [2,6,12,13]. We hypothesize that the presence of KKO will produce results characteristic of other thrombotic conditions.

2. Methods

2.1. Blood samples and the HIT model system

Samples of whole human blood were obtained using a cohort of five healthy individuals under full ethical approval and with informed written consent (REC No. 13/WA/0190). Blood was collected from the median cubital vein using a 21-gauge butterfly line (Greiner Bio One). The first few ml of blood was collected via an additive free Vacuette® and subsequently discarded in order to ensure that minimal tissue factor was present. 10 ml of blood was collected and carefully ejected into a sterile plastic universal bijou container containing no anticoagulant [14]. Samples were mixed with Unfractionated Heparin (UFH) (Sigma-Aldrich) at a therapeutically relevant concentration of 0.5 U/ml [15]. In the first part of the study, the samples were then mixed with a solution of PF4 (0 μg/ml–60 μg/ml) in Tris-buffered saline to find the optimal concentration of PF4 to bind to and neutralize the effects of UFH. Five samples of blood were used for each concentration of PF4 (n = 5). In the second part of the study, samples of blood from each of the five healthy volunteers were obtained on three separate occasions (n = 15). Samples at the PF4 concentration that neutralized the heparin effect were then prepared and divided into two aliquots. Pathogenic KKO monoclonal antibodies (100 μg/ml) were added to one aliquot and non-pathogenic RTO (100 μg/ml) monoclonal IgG antibodies, which bind to PF4 independent of heparin, were added to the other aliquot as a control [12]. 1.2 ml of each sample was used immediately for rheological analysis. 1 ml of each sample was allowed to clot in a 9 well sterile plate for imaging by scanning electron microscopy. A further 1 ml of each sample was anticoagulated using sodium citrate (3.8%), with a 1:9 ratio of citrate to blood, for flow cytometry.

2.2. Rheology

The gel point of samples was measured using an AR-G2 Rheometer (TA Instruments, UK). 1.2 ml of each sample was carefully pipetted onto a 60 mm parallel plate geometry of an AR-G2 Rheometer (TA Instruments, UK) with the lower plate controlled at a temperature of 37 °C by means of a Peltier unit. The gap was set to 380 μm, commensurate to the value of the gap used in the study of Evans et al. [14]. A low viscosity silicone oil was used to seal the sample in order to minimize evaporation at the sample edge. The values of storage moduli G' and loss moduli G'' of the sample during coagulation were monitored over a frequency range of 0.2 to 2 Hz (using four discrete frequencies) by the application of small amplitude oscillatory shear. The absence of a third harmonic response confirmed that measurements were conducted within the linear viscoelastic range (Fig. 1). At the gel point, G' and G'' exhibit a power law dependence on frequency of oscillation, and the phase angle δ ($= \tan^{-1}(G''/G')$ is frequency independent. The gel point signifies the transition from viscoelastic liquid-like behavior to viscoelastic solid-like behavior, and therefore provides an unequivocal measurement of clotting time in terms of the clot's haemostatic functionality [11,14]. Furthermore, the values of the phase angle at the gel point permits calculation of the fractal dimension, d_f, a structural parameter used to quantify the structure and complexity of the fibrin network of each sample [11,14,16,17]. In the case of the experiments involving the two antibodies, samples prepared from the same blood were tested simultaneously using two AR-G2 rheometers. Computer generated random fractal aggregates utilizing a box counting approach produced a visual illustration of the incipient clot microstructure corresponding to the experimental clots, based on the d_f obtained from rheology [18].
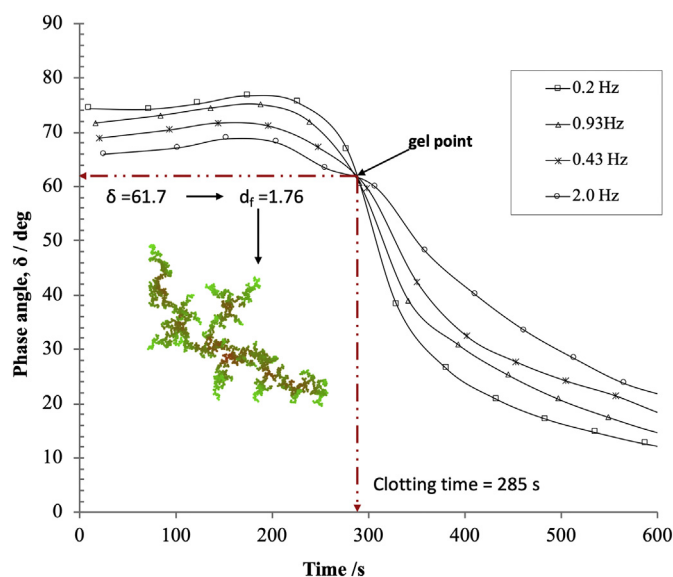

Fig. 1. Example of the results of a rheological measurement of coagulating blood. The phase angle, δ, at four different frequencies is plot as a function of time. The gel point, as detected by a frequency independent δ, indicates the transition from viscoelastic liquid-like behavior to viscoelastic solid-like behavior. The gel point provides two biomarkers of haemostasis (i) the clotting time, based on the time to reach the gel point and (ii) the fractal dimension, d_f, which can be calculated from the value of δ at the gel point, and provides a measure of the structural complexity of the clot. The image (inset) is a computer generated random fractal aggregate corresponding to the calculated value of d_f for the experimental clots.

2.3. Scanning electron microscopy

Samples were allowed to clot and prepared for microscopy and subsequent image analysis using the following procedures. To remove excess salt, the specimens were washed 3 times, in 10–20 min intervals, by permeation with 50 mM sodium cacodylate buffer solution (Spi Supplier, West Chester, PA, USA) at pH 7.4. The samples were then fixed overnight in 2% glutaraldehyde (Sigma-Aldrich Ltd., UK), after which they were washed in distilled water and then dehydrated using a series of increasing ethanol concentrations (30–100%), over a period of 3.5 h. The dehydrated samples were rinsed with 100% hexamethyldisilazane (Sigma-Aldrich Ltd., UK) solution three times and left overnight to dry. The sample was then coated with gold-palladium using sputter coating and imaged by SEM (Hitachi 4800 S, Hitachi High-Technologies Pte Ltd., Singapore). Several areas of each clot were examined before choosing fields containing the fibrin network that were most representative of those found in the entire clot. Digitized electron micrographs were taken at 10 kV at magnifications of 4000 and 10,000. The fibre diameter distribution was analysed using Image J (National Institutes of Health) by placing a random grid of crosses (500 crosses/image) on images and using the line tool to measure fibre diameter [19]. 20 images at each magnification were used to provide histograms of fibre diameter for each clot.

2.4. Flow cytometry

Citrated samples of blood (20 μl per tube) were fixed and stained with PE-conjugated anti-human CD62P (Bio-Rad Laboratories, Inc.) as a marker for platelet activation [20]. After adding antibody to the blood the samples were incubated on ice in the dark for 30 min. Red blood cells were then lysed by adding 1.5 ml of BD FACS Lysing Solution (BD Bioscience) to each sample for 10 min at room temperature followed by centrifugation at 515g at 4 °C for 10 min. Cells were then washed twice with 1.5 ml of FACS buffer (PBS, Life Technologies Ltd.,/0.2% FCS,
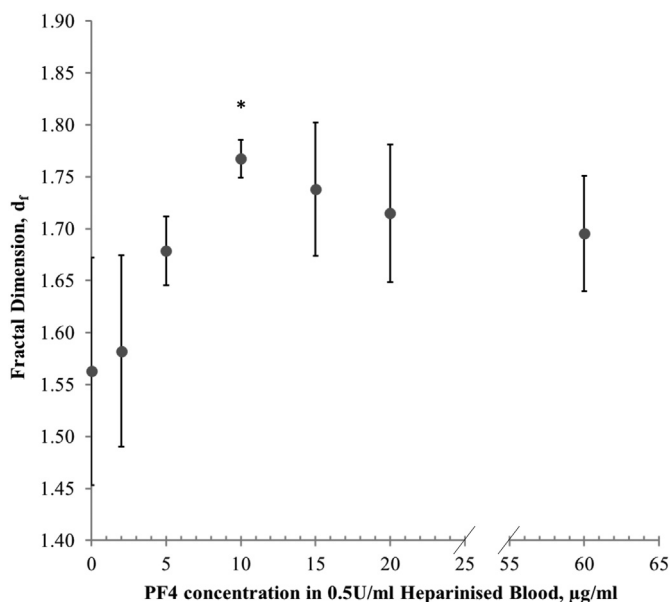
Fig. 2. The neutralization of heparin by PF4. Fractal dimension, d_f, of clots formed in heparinized blood (0.5 U/ml) with various concentrations of PF4 (0 to 60 μg/ml). The optimal concentration of 10 μg/ml, as depicted by *, produces a clot with d_f most similar to that found in whole blood from the cohort of volunteers.

Sigma-Aldrich and 0.05 sodium azide, Life Technologies Ltd.). 200 μl of BD Stabilising Fixative (BD Bioscience) was added after the second wash to each sample and stored at 4 °C overnight. A fluorescence minus one approach was used to set analysis gates [21]. Sample was treated with 4 μM of phorbol 12-myristate 13-acetate (PMA; Sigma-Aldrich) for 30 min were used as a positive control for CD62P expression [22,23].

All samples were acquired within 24 h of collection using a Beckman Coulter Navios flow cytometer with the 488 nm laser and 585/42 filter. The platelet population was gated to include both platelets in a resting and activated state using the forward scatter (FSC) and side scatter (SSC) of the unstained and positive controls as guidance and a total of 10,000 events within this gate were recorded. The data were analysed in Kaluza 1.2 (Beckman Coulter, UK). Histograms were used to report the percentage of CD62P positive activated platelet events.

3. Results and discussion

3.1. The optimal concentration of PF4 to neutralize the effects of UFH

The addition of PF4 to heparinized blood without other inhibitors (Fig. 2) revealed a characteristic bell-shaped curve similar to that seen in previous reports where PF4 modulated the antigenicity of HIT complexes [24]. The value of d_f was relatively low ($d_f = 1.56 \pm 0.108$) in heparinized blood without PF4 compared to the unadulterated blood ($d_f = 1.76 \pm 0.046$) and was similar to the value found in a previous study involving the in vitro addition of heparin [14]. The addition of increasing levels of PF4 led to a gradual increase of d_f up to a maximum value ($d_f = 1.77 \pm 0.028$) at a PF4 concentration of 10 μg/ml; further increasing levels of PF4 led to small decreases in d_f. A one-way ANOVA test revealed that a PF4 concentration of 10 μg/ml produced a value of d_f most similar (mean difference of 0.008) to that found in the unadulterated blood and also produced a d_f with the least variation. This concentration of PF4 (10 μg/ml) is the optimal required for neutralizing the effects of heparin and to promote the formation of ULCs necessary to study the effects of HIT-like antibodies (henceforth, referred as the HIT model system). Furthermore, the corresponding value of d_f (1.77 ± 0.028) is not statistically significantly different ($p = 0.26$) from the previously established healthy value (1.74 ± 0.050) [25]. The observed decrease in d_f at higher levels of PF4 may be due to excess PF4 interacting with different proteins or increasing the positive charge within the system and interfering with the coagulation process [26]. Excess amounts of PF4 have been reported to reduce the viscoelasticity of the fibrin network that forms in platelet poor plasma and platelet rich plasma, with saturating amounts of PF4 leading to a reduced porosity of the fibrin network [27].

3.2. The HIT model system

The HIT model system using PF4, heparin and the HIT pathogenic antibody KKO in whole blood revealed striking effects on clot microstructure as characterized by d_f. A significant difference ($p < 0.0001$) was found between d_f in the samples containing the pathogenic antibody KKO and the non-pathogenic or blocking antibody RTO, confirming the hypothesis that clot structure is altered in blood containing the pathogenic HIT-like antibodies (see Fig. 3a). Likewise, a significant difference was found between d_f in samples containing KKO and the neutralized samples of heparinized blood ($p = 0.008$). There was no significant difference in d_f in samples containing RTO and the unadulterated blood ($p = 0.16$). The higher d_f value observed in samples
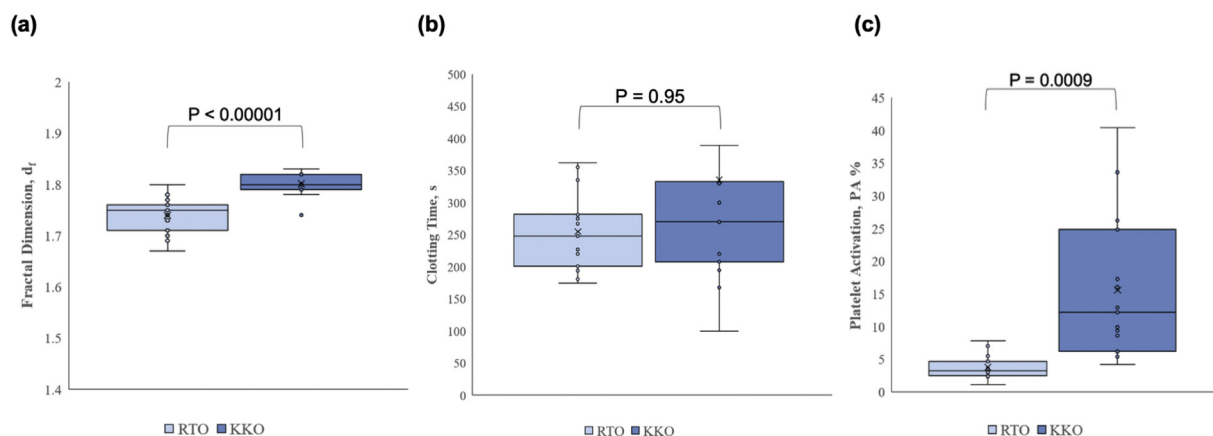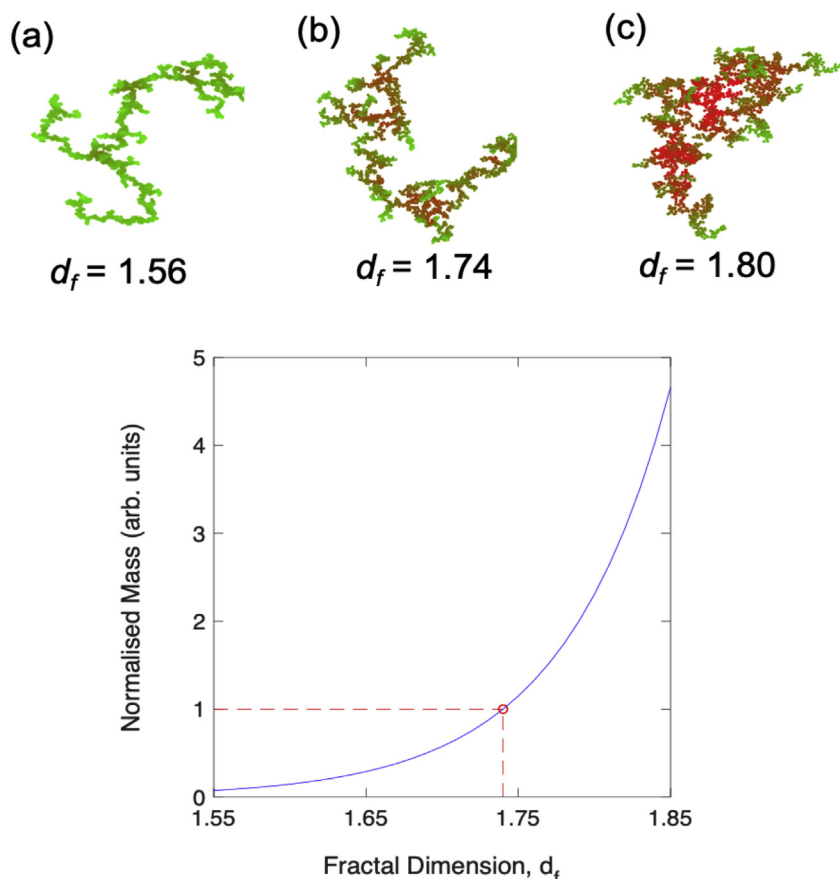

Fig. 3. The thrombotic characteristics of clots as measured by rheology and flow cytometry. Measured values of (a) fractal dimension, d_f, (b) clotting time, and (c) platelet activation, in samples of blood containing the non-pathogenic antibody RTO and the pathogenic antibody KKO (n = 15). Graphs are presented as box and whisper plots, whereby a cross represents the mean value, circles represent individual data points, the shaded box represents the values bound by the upper and lower quartile, the horizontal line represents the median value, and the bars (whiskers) represent the range. A significant difference in d_f ($p < 0.00001$) and activated platelets ($p = 0.0009$) was found between samples containing the non-pathogenic RTO and the pathogenic KKO antibodies.

Fig. 4. (upper) Illustration of the clot structures associated with the measured fractal dimensions of the clots, from computer generated random fractal aggregates corresponding to (a) heparinized blood (0.5 U/ml), d_f = 1.56, (b) heparinized blood (0.5 U/ml) with PF4 (10 μg/ml) and RTO antibodies (100 μg/ml), d_f = 1.74 and (c) heparinized blood (0.5 U/ml) with PF4 (10 μg/ml) and KKO antibodies (100 μg/ml), d_f = 1.80. The fibrin network is depicted in green with denser regions of fibrin in red. (lower) Representation of clot mass for different stages of the HIT model system. Clot mass, normalised to a d_f = 1.74 (RTO control), as a function of fractal dimension. The non-linear relationship between mass and fractal dimension illustrates that small changes in d_f requires large increases in associated clot mass. The incipient clot formed at the gel point in the samples containing KKO has an associated mass 2.5 times greater than that of the RTO counterpart. (For interpretation of the references to color in this figure legend, the reader is referred to the web version of this article.)
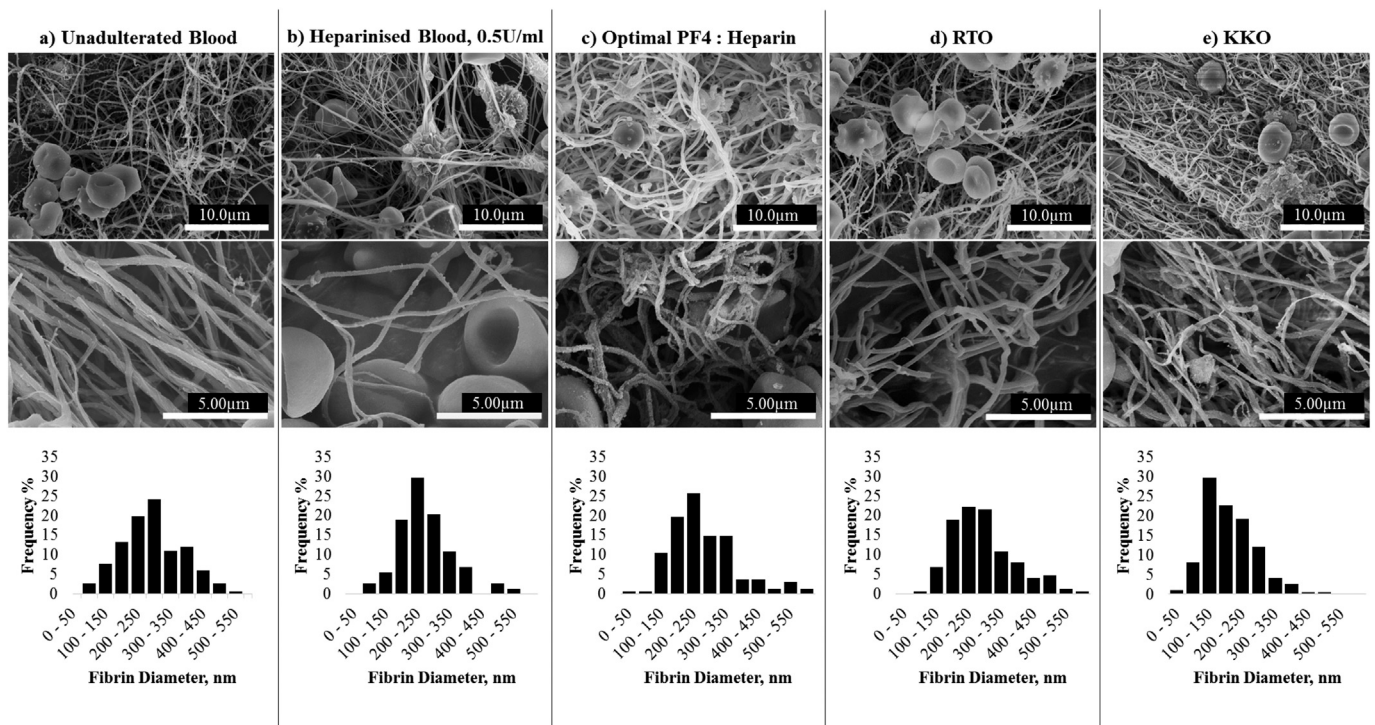
containing KKO (d_f = 1.80 ± 0.024) is characteristic of abnormal blood clots formed using blood obtained from patients with a thrombotic condition [11,25,28]. It is pertinent to note here that the relatively small differences observed in d_f correspond to large differences in associated clot mass, as demonstrated by the computational generated fractal aggregates that represent the modulation of clot structure (see Fig. 4). The incipient clot formed at the gel point in the samples containing KKO has an associated mass 2.5 times greater than that of the RTO counterpart, signifying a much denser clot that is associated with enhanced resistance to fibrinolysis [29]. Interestingly, there was no difference observed in the clotting time in samples containing KKO and RTO (p = 0.95, see Fig. 3b). In general, fibrin clots formed in shorter times produce denser clots with more mass, but such a supposition has not been fully explored and might not capture the full complexity of the coagulation process in whole blood. Furthermore, our results suggest that rate-based assays (such as activated partial thromboplastin time, prothrombin time and thromboelastography or thromboelastometry) have limited diagnostic value in the detection of thrombosis associated with HIT.

The results of the flow cytometry revealed that levels of platelet activation as measured by increased expression of CD62P were significantly greater (p = 0.0009) in samples containing KKO versus RTO (Fig. 3c) and increasing levels of platelet activation coincided with increases in d_f. These results are compatible with the notion that the presence of KKO leads to a pro-thrombotic environment, since KKO antibodies are known bind to ULCs and the FcγRIIA-receptors found on platelets, which in turn creates a thrombin burst that becomes self-perpetuating [1,3]. Examination of the results from individual samples showed that the levels of activated platelets in samples containing KKO varied considerably between each donor leading to an observed high degree of variability (illustrated in the box and whisker plot of Fig. 3c), as shown previously [30,31]. In contrast, d_f showed little variation in

the presence of KKO and was consistently elevated. Moreover, there was a small to moderate positive correlation between values of d_f and platelet activation (Pearson coefficient value, r = 0.31) in the samples containing KKO. A relatively large d_f coinciding with, in some cases, a relatively small amount of platelet activation might be explained by the interaction of the pathogenic antibody with other cells within the blood sample. For example, studies have shown that HIT-like antibodies can activate monocytes in the presence of PF4 and these activated monocytes can express tissue factor, helping in generating procoagulant activity [32].

Fig. 5 (upper) shows micrographs of blood clots formed at each stage of the HIT model system obtained using SEM. The images were selected as those most representative of the fibrin network of the entire clot. Comparison of the images show progressive changes in the structures of the underlying fibrin network, with a pattern consistent with the rheology studies in that clots with more "dense" or "tight" networks of fibrin fibres correspond to those with the largest values of d_f. The addition of heparin leads to a more "open" or more porous fibrin network (compared to the network formed in unadulterated whole blood). The addition of PF4 to the heparinized blood produces a clot fibrin network that is similar to the unadulterated blood clot. The addition of non-pathogenic anti-PF4 antibody RTO to the blood system containing heparin and PF4 did not affect the structure significantly. The images obtained from samples in the presence of HIT-like monoclonal KKO antibodies produced the most striking visual differences, showing a network consisting of a highly branched and compact arrangement of relatively thin fibrin fibres. The quantification of fibre diameter as depicted in the histograms (Fig. 5, lower) show that the presence of KKO produces clots made up of a higher proportion of thinner (< 150 nm) fibres compared to the RTO control. Clots produced with KKO consist of 36% of fibres of diameter of < 150 nm, in contrast to clots produced with RTO where 6% of fibres have diameter

Fig. 5. (upper) Micrographs of blood clots formed at each stage of the HIT model system; a) unadulterated blood, b) heparinized blood (0.5 U/ml), c) heparinized blood (0.5 U/ml) with optimal PF4 concentration, 10 μg/ml) d) heparinized blood (0.5 U/ml) with PF4 (10 μg/ml) and RTO antibodies (100 μg/ml), e) heparinized blood (0.5 U/ml) with PF4 (10 μg/ml) and KKO antibodies (100 μg/ml). The results show images of the fibrin network of the blood clot together with cellular material such as activated platelets, red and white blood cells. Visual inspection shows some differences in the underlying network between the samples. The addition of heparin leads to a more "open" or more porous fibrin network (compared to the network formed in unadulterated whole blood). The addition of PF4 to the heparinized blood produces a clot fibrin network that is similar to the unadulterated blood clot. The addition of RTO to the blood system containing heparin and PF4 produced clots with similar features to those without RTO. However, the addition of KKO to the blood system containing heparin and PF4 leads to marked differences in structure, showing a highly branched or "dense" network of thin fibrin fibres. (lower) Fibre width distribution measured from images obtained from scanning electron micrographs at each stage of the HIT model system. The presence of KKO leads to clots made up of a higher proportion of thinner (< 150 nm) fibres compared to the RTO control.

of < 150 nm. Clots formed from dense networks of thinner fibres have been consistently found in many thrombotic conditions [7–10,33,34]. Such clots are generally stiffer, have lower permeability and are more resistant to fibrinolysis than clots made up of a sparse network of thicker fibres [35,36] and are likely to contribute to the pro-thrombotic phenotype in HIT.

4. Conclusions

In summary, we have shown that the presence of the pathogenic HIT-like monoclonal antibody KKO, results in clots that are characteristic of other thrombotic conditions. These observed alterations in clot microstructure, as expressed by d_f, can be potentially exploited as a structural biomarker for the detection, management and monitoring of HIT-associated thrombosis. A future study will involve the assessment of the diagnostic and prognostic value of measuring d_f in blood obtained from patients undergoing heparin therapy.

Author contributions

K. Hawkins and J. W. Weisel designed the research, interpreted data and wrote the manuscript. B.R. Thomas designed the research, performed laboratory measurements and analysis, and wrote the manuscript. L. Rauova designed the research, provided vital reagents and revised the manuscript for important intellectual content. N. Badiei and R. J. Hambly performed laboratory measurements. M.R. Brown performed computer simulations. C. A. Thornton and P. R. Williams revised the manuscript for important intellectual content.

References

[1] M. Franchini, Heparin-induced thrombocytopenia: an update, Thromb. J. 3 (2005) 14.
[2] T.E. Warkentin, Heparin-induced thrombocytopenia: pathogenesis and management, Br. J. Haematol. 121 (2003) 535–555.
[3] A. Cuker, D.B. Cines, How I treat heparin-induced thrombocytopenia, Blood 119 (2012) 2209–2218.
[4] D.E. Golan, E.J. Armstrong, A.W. Armstrong, A.H. TashjianJr. (Eds.), Principles of Pharmacology: The Pathophysiologic Basis of Drug Therapy, 3rd ed., Lippincott Williams & Wilkins, Philadelphia, PA, 2012.
[5] C. Potschke, S. Selleng, B.M. Bröker, A. Greinacher, Heparin-induced thrombocytopenia: further evidence for a unique immune response, Blood 120 (2012) 4238–4245.
[6] L. Rauova, M. Poncz, S.E. McKenzie, M.P. Reilly, G. Arepally, J.W. Weisel, C. Nagaswami, D.B. Cines, B.S. Sachais, Ultralarge complexes of PF4 and heparin are central to the pathogenesis of heparin induced thrombocytopenia, Blood 105 (2005) 131–138.
[7] R.A.S. Ariëns, Denser matters, Blood 114 (2009) 3978–3979.
[8] J.P. Collet, Y. Allali, C. Lesty, M.L. Tanguy, J. Silvain, A. Ankri, B. Blanchet, R. Dumaine, J. Gianetti, L. Payot, J.W. Weisel, G. Montalescot, Altered fibrin architecture is associated with hypofibrinolysis and premature coronary athero-thrombosis, Arterioscler. Thromb. Vasc. Biol. 26 (2006) 2567–2573.
[9] A. Undas, K. Zawilska, M. Ciesla-Dul, A. Lehmann-Kopydłowska, A. Skubiszak, K. Ciepłuch, W. Tracz, Altered fibrin clot structure/function in patients with idiopathic venous thromboembolism and in their relatives, Blood 114 (2009) 4272–4278.

[10] A. Undas, P. Podolec, K. Zawilska, M. Pieculewicz, I. Jedliński, E. Stepień, E. Konarska-Kuszewska, P. Weglarz, M. Duszyńska, E. Hanschke, T. Przewlocki, W. Tracz, Altered fibrin clot structure/function in patients with cryptogenic ischemic stroke, Stroke 40 (2009) 1499–1501.

[11] M.J. Lawrence, A. Sabra, G. Mills, S.G. Pillai, W. Abdullah, K. Hawkins, R.H. Morris, S.J. Davidson, L.A. D'Silva, D.J. Curtis, M.R. Brown, J.W. Weisel, P.R. Williams, P.A. Evans, A new biomarker quantifies differences in clot microstructure in patients with venous thromboembolism, Br. J. Haematol. 168 (2015) 571–575.

[12] L. Rauova, G. Arepally, S.E. McKenzie, B.A. Konkle, D.B. Cines, M. Poncz, Platelet and monocyte antigenic complexes in the pathogenesis of heparin-induced thrombocytopenia (HIT), J. Thromb. Haemost. 7 (2009) 249–252.

[13] A. Cuker, A.H. Rux, J.L. Hinds, M. Dela Cruz, S.V. Yarovoi, I.A. Brown, W. Yang, B.A. Konkle, G.M. Arepally, S.P. Watson, D.B. Cines, B.S. Sachais, Novel diagnostic assays for heparin-induced thrombocytopenia, Blood 121 (2013) 3727–3732.

[14] P.A. Evans, K. Hawkins, R.H. Morris, N. Thirumalai, R. Munro, L. Wakeman, M.J. Lawrence, P.R. Williams, Gel point and fractal microstructure of incipient blood clots are significant new markers of hemostasis for healthy and anticoagulated blood, Blood 116 (2010) 3341–3346.

[15] J. Hirsh, T.E. Warkentin, S.G. Shaughnessy, S.S. Anand, J.L. Halperin, R. Raschke, C. Granger, E.M. Ohman, J.E. Dalen, Heparin and low-molecular-weight heparin: mechanisms of action, pharmacokinetics, dosing, monitoring, efficacy, and safety, Chest 119 (2001) 64S–94S.

[16] D.J. Curtis, P.R. Williams, N. Badiei, A.I. Campbell, K. Hawkins, P.A. Evans, M.R. Brown, A study of microstructural templating in fibrin–thrombin gel networks by spectral and viscoelastic analysis, Soft Matter 9 (2013) 4883–4889.

[17] D.J. Curtis, M.R. Brown, K. Hawkins, P.A. Evans, M.J. Lawrence, P. Rees, P.R. Williams, Rheometrical and molecular dynamics simulation studies of incipient clot formation in fibrin-thrombin gels: an activation limited aggregation approach, J. Non-Newton Fluid Mech. 166 (2011) 932–938.

[18] M.R. Brown, R. Errington, P. Rees, P.R. Williams, S.P. Wilks, A highly efficient algorithm for the generation of random fractal aggregates, Physica D 239 (2010) 1061–1066.

[19] N. Badiei, A.M. Sowedan, D.J. Curtis, M.R. Brown, M.J. Lawrence, A.I. Campbell, A. Sabra, P.A. Evans, J.W. Weisel, I.N. Chernysh, C. Nagaswami, P.R. Williams, K. Hawkins, Effects of unidirectional flow shear stresses on the formation, fractal microstructure and rigidity of incipient whole blood clots and fibrin gels, Clin. Hemorheol. Microcirc. 60 (2015) 451–464.

[20] T. Murakami, Y. Komiyama, M. Masuda, H. Kido, S. Nomura, S. Fukuhara, M. Karakawa, T. Iwasaka, H. Takahashi, Flow cytometric analysis of platelet activation markers CD62P and CD63 in patients with coronary artery disease, Eur. J. Clin. Invest. 26 (1996) 996–1003.

[21] L.A. Herzenberg, J. Tung, W.A. Moore, L.A. Herzenberg, D.R. Parks, Interpreting flow cytometry data: a guide for the perplexed, Nat. Immunol. 7 (2006) 681–685.

[22] C.H. Chan, I.L. Pieper, R. Hambly, G. Radley, A. Jones, Y. Friedmann, K.M. Hawkins, S. Westaby, G. Foster, C.A. Thornton, The CentriMag centrifugal blood pump as a benchmark for in vitro testing of hemocompatibility in implantable ventricular assist devices, Artif. Organs 39 (2015) 93–101.

[23] C.H.H. Chan, I.L. Pieper, C.R. Robinson, Y. Friedmann, V. Kanamarlapudi, C.A. Thornton, Shear stress-induced total blood trauma in multiple species, Artif. Organs 41 (2017) 934–947.

[24] L. Rauova, L. Zhai, M.A. Kowalska, G.M. Arepally, D.B. Cines, M. Poncz, Role of platelet surface PF4 antigenic complexes in heparin-induced thrombocytopenia pathogenesis: diagnostic and therapeutic implications, Blood 107 (2006) 2346–2353.

[25] S.N. Stanford, A. Sabra, L. D'Silva, M. Lawrence, R.H. Morris, S. Storton, M.R. Brown, V. Evans, K. Hawkins, P.R. Williams, S.J. Davidson, M. Wani, J.F. Potter, P.A. Evans, The changes in clot microstructure in patients with ischaemic stroke and the effects of therapeutic intervention: a prospective observational study, BMC Neurol. 15 (2015) 35.

[26] D.E. Eslin, C. Zhang, K.J. Samuels, L. Rauova, L. Zhai, S. Niewiarowski, D.B. Cines, M. Poncz, M.A. Kowalska, Transgenic mice studies demonstrate a role for platelet factor 4 in thrombosis: dissociation between anticoagulant and antithrombotic effect of heparin, Blood 104 (2004) 3173–3180.

[27] A.A. Amelot, M. Tagzirt, G. Ducouret, R.L. Kuen, B.F. Le Bonniec, Platelet factor 4 (CXCL4) seals blood clots by altering the structure of fibrin, J. Biol. Chem. 282 (2007) 710–720.

[28] N.A. Davies, N.K. Harrison, R.H.K. Morris, S. Noble, M.J. Lawrence, L.A. D'Silva, L. Broome, M.R. Brown, K.M. Hawkins, P.R. Williams, S. Davidson, P.A. Evans, Fractal dimension (df) as a new structural biomarker of clot microstructure in different stages of lung cancer, Thromb. Haemost. 114 (2015) 1251–1259.

[29] A. Undas, R.A. Ariëns, Fibrin clot structure and function: a role in the pathophysiology of arterial and venous thromboembolic diseases, Arterioscler. Thromb. Vasc. Biol. 31 (12) (2011) e88–e99.

[30] T.E. Warkentin, C.P.M. Hayward, C.A. Smith, P.M. Kelly, J.G. Kelton, Determinants of donor platelet variability when testing for heparin-induced thrombocytopenia, J. Lab. Clin. Med. 120 (1992) 371–379.

[31] T.E. Warkentin, D.M. Arnold, I. Nazi, J.G. Kelton, The platelet serotonin-release assay, Am. J. Hematol. 90 (2015) 564–572.

[32] L. Rauova, J.D. Hirsch, T.K. Greene, L. Zhai, V.M. Hayes, M.A. Kowalska, D.B. Cines, M. Poncz, Monocyte-bound PF4 in the pathogenesis of heparin-induced thrombocytopenia, Blood 116 (2010) 5021–5031.

[33] J.W. Weisel, Structure of fibrin: impact on clot stability, J. Thromb. Haemost. 5 (2007) 116–124.

[34] A.S. Wolberg, R.A. Campbell, Thrombin generation, fibrin clot formation and hemostasis, Transfus. Apher. Sci. 38 (2008) 15–23.

[35] J.W. Weisel, R.I. Litvinov, Mechanisms of fibrin polymerization and clinical implications, Blood 121 (2013) 1712–1719.

[36] J.P. Collet, D. Park, C. Lesty, J. Soria, C. Soria, G. Montalescot, J.W. Weisel, Influence of fibrin network conformation and fibrin fiber diameter on fibrinolysis speed: dynamic and structural approaches by confocal microscopy, Arterioscler. Thromb. Vasc. Biol. 20 (2000) 1354–1361.